Journal of Applied Physics

RESEARCH ARTICLE | NOVEMBER 13 2023

Influence of moisture on the ferroelectric properties of sputtered hafnium oxide thin films

Fenja Berg ; Nils Kopperberg ; Jan Lübben ; Ilia Valov ; Xiaochao Wu ; Ulrich Simon ; Ulrich Böttger

J. Appl. Phys. 134, 185106 (2023)
https://doi.org/10.1063/5.0171345

Journal of Applied Physics ARTICLE pubs.aip.org/aip/jap

Influence of moisture on the ferroelectric properties of sputtered hafnium oxide thin films

Cite as: J. Appl. Phys. **134**, 185106 (2023); doi: 10.1063/5.0171345
Submitted: 8 August 2023 · Accepted: 21 October 2023 ·
Published Online: 13 November 2023

Fenja Berg,[1,a)] Nils Kopperberg,[1] Jan Lübben,[1] Ilia Valov,[2] Xiaochao Wu,[3] Ulrich Simon,[3] and Ulrich Böttger[1]

AFFILIATIONS

[1]Institute of Materials in Electrical Engineering and Information Technology 2, RWTH Aachen University, Aachen, Germany
[2]Peter Gruenberg Institute 7, Research Centre Jülich, Jülich, Germany
[3]Institute of Inorganic Chemistry, RWTH Aachen University, Aachen, Germany

[a)]**Author to whom correspondence should be addressed:** f.berg@iwe.rwth-aachen.de

ABSTRACT

While the influence of various fabrication parameters during deposition on the ferroelectricity of hafnium oxide has been extensively studied, the effect of different atmospheres on the actual switching process has not yet been investigated. In this work, we characterized the ferroelectric properties of undoped hafnium oxide prepared by reactive sputtering under three different atmospheres: dry oxygen/nitrogen, wet nitrogen, and vacuum conditions. We found a significant correlation between dry and wet atmospheres and resulting polarization. Specifically, we observed a direct effect on ferroelectric switching when the film was exposed to dry atmospheres and vacuum, resulting in a higher electric field necessary to initialize the wake-up effect due to an initial imprint effect. Increasing the amount of wet nitrogen during switching decreased the imprint and lowered the necessary voltage required for the wake up. We present a simple model that explains and discusses the incorporation of moisture and its resulting consequences on the ferroelectric properties of hafnium oxide. Additionally, kinetic Monte Carlo simulations showed that the addition of protons to the oxide thin film leads to a lowering of the potential and to a redistribution of protons and oxygen vacancies, which reduces the initial imprint.

I. INTRODUCTION

Integrated thin films of ferroelectric hafnium oxide, reported by Boeschke *et al.* in 2011,[1] are promising candidates to overcome the drawbacks of conventional lead zirconate titanate (PZT) films, such as lack of CMOS compatibility and scalability.[2,3] The ferroelectricity in hafnium oxide is attributed to a non-centrosymmetric orthorhombic phase, which coexists with the known monoclinic, cubic, and tetragonal phases.[4,5] In 2018, a rhombohedral phase was reported in epitaxial thin hafnium zirconium oxide (HZO) thin films, which also stabilizes the ferroelectric properties.[6,7] For doped as well as undoped hafnium oxide, initial electrical cycling (the wake-up effect) plays an important role in stabilizing the ferroelectric phase by increasing the remanent polarization and opening a constricted hysteresis which is often observed in the pristine state.[8,9] This effect is mostly explained by a field-driven redistribution of oxygen vacancies, which decreases an initially present built-in bias field and supports domain wall depinning within the layer. The defect redistribution is often observed to be accompanied by a field-driven phase transition to the ferroelectric orthorhombic phase.[10–14] With further cycling the remanent polarization decreases again, known as the Fatigue effect, which has also been observed in conventional ferroelectrics like PZT.[15,16] For undoped hafnium oxide, it has been reported that the influence of oxygen during deposition and annealing conditions is significant and directly affects the ferroelectric phase fraction and performance.[17–20] However, the effect of different atmospheres, especially the effect of dry or humid atmospheres, during the wake-up process has not been investigated yet. It has been shown in the literature that moisture can significantly affect the electrical properties, especially in terms of resistive switching effects and conductivity for amorphous hafnium oxide films.[21]

In this paper, we report on detailed investigations and analysis of the influence of humidity on the ferroelectric characteristics of

undoped hafnium oxide (HfO_x) for the first time. We conducted measurement series in vacuum, in mixed dry oxygen/nitrogen, dry pure nitrogen atmosphere, and at different moisture partial pressures. While dry oxygen/nitrogen atmospheres, as well as vacuum, appear to prevent or delay the wake-up effect and lead to a reduced remanent polarization at the same applied field, the addition of moist nitrogen during the switching process leads to the usual wake-up effect and the formation of hysteresis, which has already been observed several times during measurements under ambient conditions.

We found a strong initial imprint effect due to internal fields that shifts the hysteresis along the voltage axis in one direction. With a positive voltage applied to the top electrode, the voltage shift is negative, shifting the coercive voltage in both positive and negative directions to lower voltages. Increasing the moisture content decreases the imprint and the internal field and results in the common observed wake-up effect. In vacuum, a higher applied electrical field can compensate for the increased coercive voltage, leading to ferroelectric switching. In this work, a model for the influence of moisture on the internal bias field and coercive voltage is discussed. Kinetic Monte Carlo (KMC) simulations are applied to further investigate the effect of protons on the potential and, thus, the internal field responsible for the imprint.

II. EXPERIMENTAL DETAILS

The investigated film is prepared by reactive sputtering from a 1 in. metallic hafnium target at room temperature. The stack consists of a 30 nm platinum bottom electrode, a 25 nm thick HfO_x layer, and a 50 nm platinum top electrode. Hafnium oxide is sputtered at an oxygen flow of 0.28% and a process pressure of 0.002 mbar at a constant power of 40 W. The platinum bottom electrode is prepared by sputtering at 150 °C, the top electrode at room temperature. The annealing procedure is performed in a rapid thermal annealing chamber (RTA) in nitrogen atmosphere at a temperature of 600 °C and with a 30 s holding time and a 10 s ramp. The process parameters have been examined before in Ref. 22.

The structural properties were investigated by Grazing Incidence X-ray Diffraction (GI-XRD) measurements with a Panalytical MPD Pro system. A Cu-K_α wavelength from a copper x-ray tube is used to perform the measurements.

The electrical hysteresis characterization is performed with a Keithley 4200 at a frequency of 1000 Hz. The wake-up pulses are implemented as square pulses, the hysteresis measurement is done by triangular pulses. For the wake-up investigations, the pristine state of the cell was recorded before any wake-up pulse was applied. The number of wake-up cycles can be increased arbitrarily from 1 to 10^7 cycles.

The humidity during the hysteresis and wake-up measurements were measured with an analog humidity sensor. Diffuse Reflectance Infrared Fourier Transform Spectroscopy (DRIFTS) measurements were carried out with a VERTEX 70 FT-IR spectrometer from Bruker and Harrick Praying Mantis mirror system. Therefore, the HfO_x sample was deposited on silicon dioxide (SiO_2), and the SiO_2 wafer was positioned on a ceramic sample holder with a resistive heating element at the back side for temperature control. The SiO_2 substrate was fixed to the ceramic sample holder by using conductive silver paste (PLANO GmbH) for heat conduction between the heating element and the substrate. A sketch of the ceramic sample holder and the measurement setup can be seen in Fig. S1 in the supplementary material. The ceramic substrate and the HfO_x film were annealed for several hours at 120 °C in order to eliminate contributions from the silver paste in the following measurements. The temperature was chosen lower than the used crystallization temperature (600 °C) and the subsequent annealing temperature (170 °C) used in the electrical experiments to avoid affecting or changing the HfO_x film and to provide the same experimental conditions. Afterward, the ceramic substrate was placed inside a high-temperature reaction chamber (HVD-DRP, Harrcik Scientific Products, Inc.) for *in situ* measurements. The temperature of the ceramic substrates was controlled via the back-side resistive circuit and a sourcemeter (Keithley). During the whole measurements, a dry nitrogen atmosphere with a flow rate of 20 ml/min^{-1} was applied. The thin film was heated at 30 °C for 30 min, and the spectrum was recorded as background and subtracted from the spectra collected afterward. Then, the thin film was heated up to 390 °C gradually. The temperature steps amount to 20 °C and each temperature was held for 15 min. The spectra were collected with the wavenumber range of 800–4000 cm^{-1} simultaneously.

Leakage current measurements were performed with a Keithly6430 and an additional current amplifier from Femto. The sweep rate was chosen to 0.8 V/min.

III. RESULTS AND DISCUSSION

For a structural characterization of the thin HfO_x film GI-XRD measurements were carried out. HfO_x thin films tend to crystallize in a combination of the tetragonal, the ferroelectric orthorhombic, and the monoclinic phase. However, the similar peak positions of the tetragonal and orthorhombic phases make them indistinguishable using GI-XRD alone. Therefore, we only differentiate between the monoclinic and non-monoclinic phases.

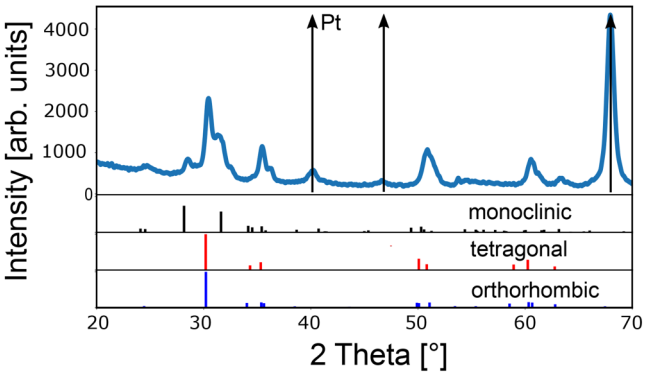

FIG. 1. GI-XRD measurement of the investigated thin HfO_x film. The crystal structure is indicated by the reference XRD pattern below. The diffraction peaks belonging to the platinum bottom and top electrode are marked by arrows.

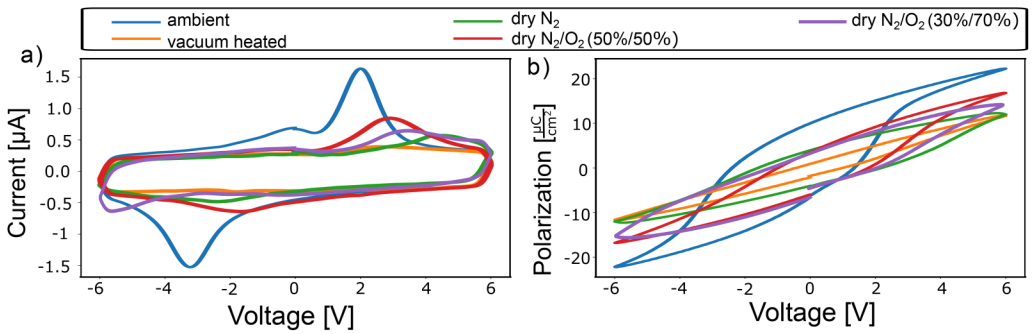

FIG. 2. (a) Current measurements in ambient atmosphere, in vacuum after additional heating, and in dry oxygen and nitrogen atmosphere. (b) Corresponding hysteresis.

The crystal structure in Fig. 1 reveals a mixed phase consisting of a small monoclinic and a larger non-monoclinic phase fraction. For identifying the platinum (Pt) peaks, a reference GI-XRD measurement of the Pt electrode on SiO_2 is shown in Fig. S2 in the supplementary material.

In Ref. 22, a similar prepared HfO_x thin film was characterized by further measurement methods and an orthorhombic/tetragonal phase with some monoclinic phase content was found. The high non-monoclinic phase fraction in the GI-XRD measurement indicates good ferroelectric properties and a high remanent polarization.

A. Effects of different atmospheres

Further electrical measurements were performed to characterize the ferroelectric properties under different atmosphere conditions in a vacuum chamber which enables the control of the supply of moisture and the carrier gases: oxygen (O_2) and nitrogen (N_2). To create equal conditions, the different atmospheres were introduced according to the following scheme: (i) The normal investigated state in ambient atmosphere without evacuating the chamber, (ii) the evacuated state at 7×10^{-6} mbar after 12 h evacuation. In some cases, the sample had to be heated (170 °C for 1 h) by an additional annealing element underneath the sample holder to achieve the chamber pressure. (iii) The dry state after evacuation, which was established by subsequent venting of the chamber by pure dry nitrogen or a mixture of 50% dry nitrogen and 50% dry oxygen or 30% nitrogen and 70% oxygen. The relative amount of residual humidity did not exceed 4%. (iv) The wet state, which resulted from afterward addition of wet nitrogen with different amounts of humidity between 27% and 70% into the chamber. It should be noted that the vacuum chamber was evacuated every time before being filled with the different atmospheres or wet nitrogen. The corresponding current and hysteresis measurements for ambient atmosphere (i), vacuum (ii), and dry atmospheres (iii) are shown in Figs. 2(a) and 2(b), respectively. For all measurements, a wake up of 1000 cycles was performed.

The prepared ferroelectric hafnium oxide thin film has a $2P_r = P_{r,+} - P_{r,-}$ polarization value of about 18 µC/cm² when the hysteresis measurement is performed in ambient air (scenario i). In vacuum, however, the characteristic ferroelectric switching peaks [see Fig. 2(a)] have almost completely disappeared and no hysteretic behavior is measured. When the vacuum is broken by adding dry nitrogen or a mix of dry nitrogen/oxygen, the measured relative humidity increases about time to a maximum humidity of 4% due to the fact that the supplied gases are not completely dry coming out of the supply lines. With the slight increase in humidity, a small increase in polarization is recognizable, which is enhanced compared to dry nitrogen when additional dry oxygen is added to the atmosphere. However, the polarization is still significantly reduced compared to measurements taken in ambient atmosphere.

Under vacuum, the remanent polarization seems to decrease the most, followed by dry nitrogen and a mixture of dry nitrogen and oxygen. However, the largest remanent polarization can be observed in ambient atmosphere leading to the conclusion that the moisture content of the environment seems to have a decisive influence on the ferroelectric properties. For detailed studies, investigations in humid atmospheres were carried out in a further experiment. For statistical reasons, several measurements were taken for each different humidity content and plotted in a boxplot in Fig. 3. The remanent polarization is extracted after a wake up of

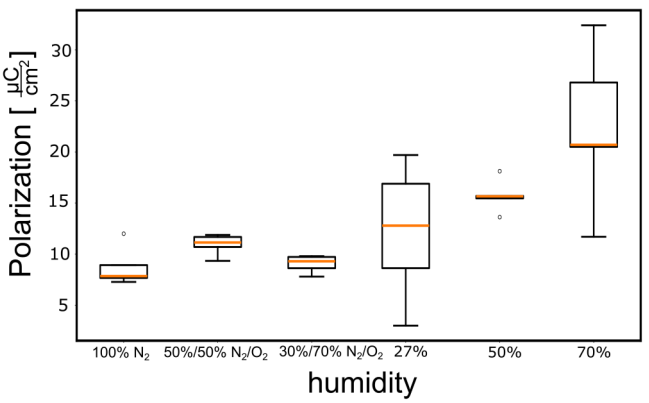

FIG. 3. Boxplot of polarization measured in different pH_2O partial pressures and in dry oxygen and dry nitrogen atmosphere with a relative humidity of 4%.

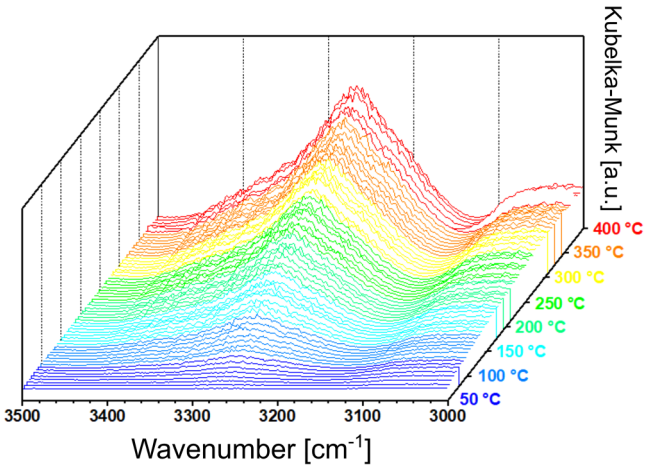

FIG. 4. *In situ* temperature programmed DRIFTS measurements of thin HfO_x. The O–H band is located between 3000 and 3300 cm^{-1}.

1000 cycles. In the boxplot diagram, the median polarization is marked red, the box contains each 25% larger and 25% smaller measurement values than the median.

The addition of moisture during the switching process results in the formation of ferroelectric hysteresis with average remanent polarization values between 12 (27%), 16 (50%), and 20 $\mu C/cm^2$ (70%). There is a dependence of polarization on the moisture content of the atmosphere since it increases significantly with the increasing moisture content. The remanent polarization for switching in dry atmosphere amounts to comparatively lower values of 8, 9, and 11 $\mu C/cm^2$.

B. Diffuse reflectance infrared Fourier transform spectroscopy measurement

From the measurements, we have concluded that moisture plays an important role during the actual ferroelectric switching process and promotes it. We performed DRIFTS measurements, which provide information about the presence of water on the surface of the thin films. The DRIFTS spectrum is converted in Kubelka–Munk units to achieve a linear dependency of the intensity on the amount of adsorbed species.[23–25] The temperature programmed spectra in the range of 3000–4000 cm^{-1} are shown in Fig. 4. The characteristic broad bands at about 3250 cm^{-1} are observed, which can be assigned to the OH stretching modes.[26–28] An increase in the band intensity at the OH related wavenumber with increasing temperature is recognizable, indicating that OH species are detected from the surface or from surface-near regions of the HfO_x film.

Similar infrared spectroscopy measurements have been conducted in previous research on crystalline HfO_x-based films,[28–30] where the OH signal was assigned to OH groups incorporated into the thin film due to exposure to humid ambient air.[28]

Further confirmation that water plays an important role could be seen in Fig. S3 in the supplementary material, which shows the hysteresis measurement of a sample heated in vacuum at 170 °C for 1 h compared to that of one without additional heating in vacuum. While the sample that was heated shows no apparent ferroelectric switching behavior, the sample measured in vacuum without additional heating exhibits a polarization of 5 C/cm^2. This decrease of remanent polarization with heating is a further strong indication that water plays an important role in our thin films during switching events.

C. Wake-up effect

In Fig. 5, we show the temporal development of the switching current in vacuum, 27% humidity, 50% humidity, and 70% humidity for different numbers of wake-up cycles along with the excitation voltage applied to the top electrode. Figure 5(a) presents the switching current in vacuum for the pristine state, after 50, 600, and 1500 cycles. No switching peaks can be detected after 50 and 600 cycles. In 1500 wake-up cycles, a small increase in switching current is observed when a positive voltage is applied while no switching peak occurred for a negative applied voltage. In Figs. 5(b)–5(d), the measurements for 27%, 50%, and 70% humidity are shown. In contrast to vacuum, measurements in humid atmospheres show significant ferroelectric switching current peaks after 50–1500 wake-up cycles.

Analyzing the change in the positions of the switching peaks with time, we find that in general, the negative coercive voltage in humid atmosphere shifts to smaller absolute voltage values with increasing cycling. For the positive coercive voltage, however, a shift to higher absolute voltages is observed. For a detailed investigation, in Fig. 6(a), the coercive voltage as well as the asymmetry of positive and negative coercive voltage $\Delta V = V_{(c,+)} + V_{(c,-)}$ are extracted. At 27% humidity and 50 wake-up cycles, the negative coercive voltage is about −5 V while the positive coercive voltage is absolutely much lower at 1.9 V, resulting in a large difference ΔV. With increasing number of cycles, negative and positive coercive voltage values are approaching each other, resulting in a decrease in voltage shift from −2.7 to −1.34 V at 1500 cycles. A similar trend can be seen for 50% and 70%. At higher humidity levels, however, the voltage asymmetry is less pronounced and voltage peaks are even visible in the pristine state, indicating that the film is already in a partly woken up state. Thus, increasing the amount of humidity results in a smaller voltage shift.

Based on the observation of the wake-up effect, we conclude that a strong asymmetry of the coercive voltage is present in the pristine state that is linked to an internal bias field. In case of the reverse of the external field, the coercive voltage shifts in the other direction (compare Fig. S4 in supplementary material), i.e., to higher absolute positive voltages and smaller absolute negative voltages, which confirms our assumption. Bias fields in thin hafnium oxide layers have been reported before and can result from an asymmetric distribution of oxygen vacancies which accumulate at the electrode oxide interface. The resulting imprint behavior has been discussed and experimentally observed before in Refs. 31and 32.

As the number of cycles during wake-up increases, the bias field is reduced, leading to an incipient wake-up effect and ferroelectric switching. In vacuum, on the other hand, no distinct ferroelectric switching can be observed after 1500 cycles. The imprint effect is so pronounced that the applied voltage is not sufficient for

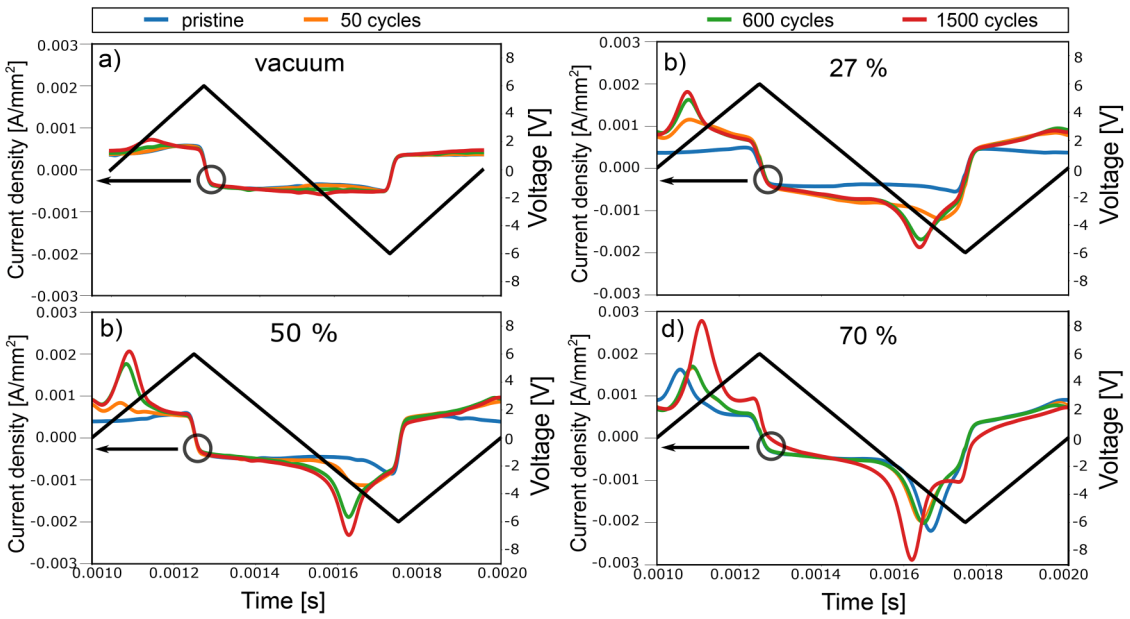

FIG. 5. Time development of the switching current in dependence of electrical cycling. Measurements taken in (a) vacuum, (b) 27% humidity, (c) 50% humidity, and (d) 70% humidity.

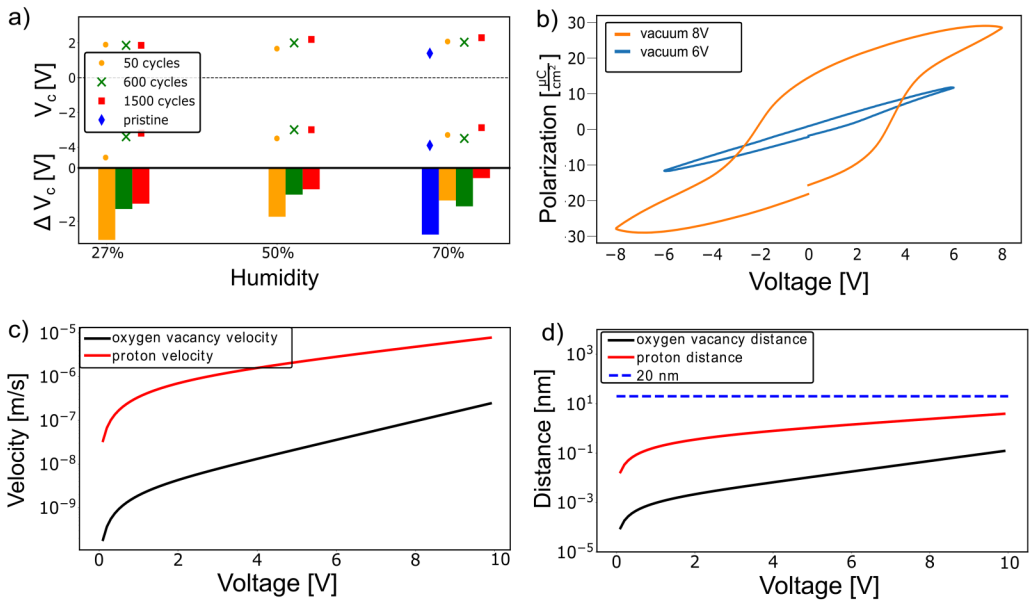

FIG. 6. (a) Development of coercive voltage for different wake-up cycles and different amounts of humidity (upper part). Asymmetry of the switching peaks as voltage shift (lower part). (b) Hysteresis measured in vacuum for 6 and 8 V excitation voltage. (c) Oxygen vacancy and proton velocity calculated by the Mott–Gurney equation. (d) The distance covered by protons and oxygen vacancies as a function of the applied voltage calculated for a time of 0.5 ms.

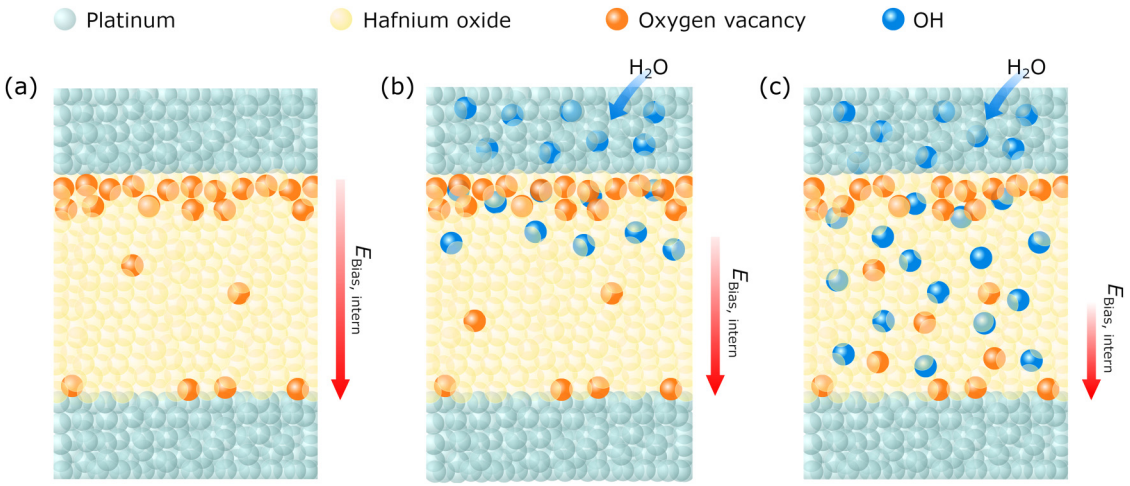

FIG. 7. (a) Pristine state: oxygen vacancies are accumulated at the top interface resulting in an internal bias field directed from the top electrode to the bottom electrode. (b) Electrical cycling in wet atmosphere leads to an incorporation of protons and OH^- via Eq. (1). (c) Further electrical cycling leads to a redistribution of protons, which further reduces the bias field.

a polarization reversal. An enhancement of the applied voltage repeals this restriction and leads to ferroelectric switching even under vacuum conditions [compare Fig. 6(b)]. It should be taken into account that the higher applied electric field leads to a rise in the leakage current.

D. Model explanation

In the following, we present a model explanation for the observed different behavior in wet and dry atmospheres. We suppose that the observed imprint effect due to the bias field present in the pristine state is caused by fabrication issues. In Ref. 33, it has been shown that annealing of HfO_x films with platinum top electrodes favors the formation of oxygen vacancies in oxygen-poor atmospheres. Consistently, we claim that for our samples annealed in pure nitrogen atmosphere oxygen vacancies accumulate at the interface between the hafnia film and the Pt top electrode forming an internal bias field across the oxide film [see Fig. 7(a)].

The reduction of the internal bias field and the imprint is attributed to a redistribution of defects in the thin film as it has been reported for oxygen vacancies during the wake up in Ref. 10. Since moisture enhances, accelerates, or even enables the reduction of the bias field, we assume that not only oxygen vacancies play an important role in decreasing the imprint effect, but that hydroxide ions have a strong impact on the bias field, especially when lower fields are applied. Therefore, the chemical processes that could occur during switching in the presence of H_2O molecules are discussed below. In Refs. 21, 34, and 35, it has been shown that moisture has a crucial impact on crystalline and amorphous oxide layers. In dense crystalline materials, the incorporation of moisture can occur at the grain boundaries due to the chemical potential gradient by the dissolution of water into OH^- and H^+ via the following equation using the Kroeger–Vink notation:

$$H_2\,O(g) + V_{\ddot{O}} + O_O^x \rightarrow 2OH_O^{\cdot}. \quad (1)$$

According to equation (1), $V_{\ddot{O}}$ refers to a twofold positively charged oxygen vacancy in relation to the lattice, O_O^x is the neutral oxygen ion on its regular lattice position, and $OH^{\cdot}$ represents a single positively charged proton sited on an oxygen ion. In the presence of moisture, one oxygen vacancy is occupied by an OH^- ion and a proton is bonded to an oxygen atom on an oxygen site resulting in two single positively charged $OH^{\cdot}$ ions relative to the lattice.

When the film is exposed to humid air, we assume that the OH^- is adsorbed and incorporated into thin film. Subsequently, OH^- is accumulated at the top interface of the film [cf. Fig. 7(b)]. When an external electric field is applied, the protons may begin to redistribute within the HfO_x layer which will be discussed in the following.

In the literature, few information about the mobility of hydrogen species in HfO_x is available. However, for yttrium stabilized zirconium oxide (YSZ), different studies of proton mobility have been reported. In Ref. 36, it was found that the grain boundaries of nanocrystalline YSZ are conductive for proton transport at room temperature. With increasing temperature, conduction is reduced due to desiccation. The calculation of activation energies for proton mobility at the grain boundaries of crystalline YSZ exhibits values between 0.03 and 1.7 eV, depending on the chosen path of the proton.[37] Under the influence of an electric field, we suppose that protons hop from one oxygen ion to another and migrate through the crystal, which leads to a more uniform distribution of the positively charged protons and to a reduction of the internal bias field. Since a higher field is necessary for the redistribution of charges without moisture present, we conclude that protons are more mobile than oxygen vacancies, which leads to a faster decay of the internal field.

In Ref. 13, the velocity of oxygen vacancies during the wake-up effect has been approximated by the Mott–Gurney equation[38]

$$v = 0.5 \cdot af \exp\left(-\frac{W_0}{K_b T}\right) \sinh\left(\frac{za}{2K_B T} E\right), \quad (2)$$

where W_0 is the activation energy, a is the hopping distance, f the attempt frequency, z the ion's charge, and E the electric field. Using values measured by Zafar *et al.*[39] ($a = 0.25$ nm, f $= 1 \times 10^{14}$ s^{-1}, $z = 2$) and an activation energy of 0.75 eV for oxygen vacancies (activation energies between 0.7 and 0.85 eV have been reported[40,41]), as well as an activation energy of 0.6 eV and $z = 1$ for protons (activation energies have been measured between 0.5 and 0.6 eV for YSZ[42,43]), the velocities at room temperature $T = 295$ K are illustrated in Fig. 6(c) as a function of applied voltage. Considering that the AC-voltage is applied for 0.5 ms for each polarity using a frequency of 1 kHz, the migration distance can be calculated in dependence of the electric field and the results are shown in Fig. 6(d). A strong dependence of the velocity on the applied voltage is evident. When the internal bias field is aligned in the same direction as the external field, the effective field $E_{int} + E_{ext}$ driving the ions is larger than in the opposite direction. Therefore, the velocity of protons and oxygen vacancies is enhanced in the direction of the bias field resulting in a net drift from the top electrode to the bottom electrode. Due to the smaller activation energy, the velocity is larger for protons compared to oxygen vacancies. After the protons have been incorporated into the interface in the hafnium oxide layer [see Fig. 7(b)], the protons start to redistribute uniformly within the oxide layer under the AC field leading to a reduction of the internal field and a lowering of the coercive voltage for the opposite direction [see Fig. 7(c)]. This is also reflected in the electrical hysteresis measurements [cf. Fig. 6(a)], where only the application of an external field leads to a lowering of the bias field over time and subsequently to the uniform migration of protons within the oxide. Moreover, Fig. 6(a) also strongly suggests that an increase in humidity level leads to more incorporated protons resulting in a faster reduction of the internal bias field. At this point, we would like to point out that the applied fabrication process results in an accumulation of twofold positively charged oxygen vacancies at the top electrode during the annealing step in nitrogen. This inhomogeneous distribution forms the ascribed bias field from top to bottom electrode. Modifications of the fabrication process may lead to a different oxygen vacancy distribution in the film and, therefore, to different orientations of the bias field, e.g., from bottom to top electrode. In this case, the redistribution of protons from the top interface into the layer would be reduced and external fields, which are higher as for the vacuum state, would have to be applied to observe ferroelectric switching. However, such a behavior was not observed in any of our prepared samples.

E. Influence of oxygen on the bias field

From the literature, it is known that oxygen can also be incorporated into crystalline solids by the following equation:[44]

$$O_2(g) + 2V_O^{\cdot\cdot} \rightarrow 2O_O^x + 4h^{\cdot}, \quad (3)$$

where $O_2(g)$ is oxygen in the gas phase, $V_O^{\cdot\cdot}$ a twofold positively charged oxygen vacancy, O_O^x is a neutral oxygen atom on its regular lattice position, and $h^{\cdot}$ is a positively charged hole with respect to the lattice.

Consequently, the incorporation of oxygen at an oxygen vacancy site could lead to a decrease in the oxygen vacancy concentration at the interface and to a reduction of the observed bias field. In addition, in Fig. 2(a), dry oxygen atmosphere seems to lead to a decrease of the coercive voltage compared to dry nitrogen atmosphere.

However, our experimental observations that the influence of humidity on the remanent polarization is significantly enhanced compared to dry oxygen atmosphere suggest that the incorporation of oxygen is less favored compared to the incorporation of OH^- from humid atmospheres. This observation is supported by further analysis. First, no real difference can be observed between 50% and 70% oxygen after 1000 wake-up cycles in terms of remanent polarization and coercive field apart from statistical fluctuations (cf. Fig. 2).

In addition, studies of the wake-up effect as a function of electrical cycling in 70% oxygen atmosphere (shown in Fig. S5 in the supplementary material) have shown that, in contrast to humid atmospheres (cf. Fig. 5), no real differences in the coercive field and switching peaks can be detected with an increasing number of cycling. This observation indicates that oxygen is not further incorporated during the actual switching event. Furthermore, similar to vacuum conditions, a higher excitation voltage is required to increase the remanent polarization (compare Fig. S6 in the supplementary material).

In the literature, reports about the incorporation of OH as well as the incorporation of oxygen can be found.[21,45–47] However, the incorporation of oxygen into hafnium oxide has been described only for temperatures significantly higher than room temperature, which are experimental conditions that were not met in our work. Therefore, oxygen incorporation during the ferroelectric switching process seems to be negligible in our case.

F. Kinetic Monte Carlo simulation

To underline our model idea that we introduced before, we developed a simple one-dimensional kinetic Monte Carlo (1D KMC) simulation model. With the help of this simulation model, we were able to investigate the influence of oxygen vacancies and protons, as well as their movement, on the electrical potential in the HfO_x thin film. The electrical potential is directly connected with the local electric field, which is responsible for the imprint mechanism in ferroelectric HfO_x films. Since our model is based on an internal bias field that is reduced in the presence of protons, we have attempted to test our model theory by appropriate simulations. The central part of our simulation model is a 25 nm thick film of HfO_x with a width of 25 m in each direction, sandwiched between two identical electrodes. The thickness and electrode sizes are similar to the experimental conditions. The oxide film is divided into 50 identical layers of 0.5 nm length each, which corresponds to the typical lattice constant and so to the diffusion lengths of ions in HfO_x.[41] Each layer can consist of a specific number of twice positively charged oxygen vacancies and singly

positive charged protons. In order to obtain the electrical potential, the one-dimensional Poisson equation

$$\frac{\partial^2 \Phi(x)}{\partial x^2} = -\frac{\rho(x)}{\varepsilon_0 \varepsilon_r} - V_{ext}(x) \tag{4}$$

is solved, where the charge density $\rho(x)$ can be calculated by the number of defects in each layer, the permittivity ε_r is known from the literature,[48] and $V_{ext}(x)$ is the externally applied voltage at the top electrode ($x = 0$). As we are interested in the time evolution of the defects and their effect on the electrical potential, we calculate transition rates for the defects jumping from one layer forward or reverse to a neighboring layer via the Mott–Gurney law[49,50]

$$R^{f/r} = N \cdot f \cdot \exp\left(-\frac{\Delta W_A^{f/r}}{k_B T}\right), \tag{5}$$

where the effective hopping barrier is modulated depending on the local potential difference between the two layers via

$$\Delta W_A^{f/r} = \Delta W_A \mp z \cdot \frac{\Delta \Phi}{2}. \tag{6}$$

Here, N denotes the number of defects (oxygen vacancies or protons) per layer, f is the attempt frequency, ΔW_A is the activation energy, and z is the charge of oxygen vacancies or protons. Finally, randomly but weighted by the transition rates, one of the processes is chosen, fulfilled, and the simulation time is updated via

$$t_{jump} = -\frac{\ln r_1}{\Sigma R}, \tag{7}$$

with r_1 being a random number between 0 and 1. All parameters used in the simulation are given in Table I.

As sketched in Fig. 7 before, we expect oxygen vacancies close to the top electrode to be responsible for an internal bias field leading to a locally reduced applied electric field and a hindered ferroelectric switching. Thus, we place oxygen vacancies into HfO_x with a linearly decreasing number from the top electrode to a distance of 5 nm. Subsequently, simulations are performed without an applied external field to determine a possible redistribution of oxygen vacancies and protons. During simulations, oxygen vacancies slightly resort and move even closer to the electrodes. The same procedure was done for a starting configuration, where 25% of the oxygen vacancies were replaced by each two protons and which showed similar results. The shape of the potential caused by the charge carrier distribution hinders protons and oxygen vacancies to redistribute uniformly within the oxide without an external field applied. The final state, which has established after time is then relatively stable without external influences and is used as the starting point for the following simulations.

TABLE I. Simulation parameters.

Symbol	Value	Symbol	Value
ΔW_A (ox. vac.)	0.75 eV	T	300 K
ΔW_A (proton)	0.6 eV	ε_r	30
z (ox. vac.)	+2	f	2×10^{13} Hz
z (proton)	+1		

In Fig. 8(a), the potential of this starting configuration (identical for both cases) is shown in the dark blue curve. Resulting from the charged ions, a potential difference of approx. 2.5 V is generated from close to the top electrode to the bottom electrode. This potential difference would strongly reduce an externally applied field and so hinder the ferroelectric switching in one direction. Furthermore, we applied an AC voltage with a frequency of 1 kHz and an amplitude of 6 V to the top electrode for both cases, with and without protons. The number of cycles was set to 100, at which ferroelectric switching peaks begin to develop experimentally in humid atmosphere (see Fig. 5). Whereas in the scenario without protons no big changes occur as can be seen in the black dashed line in Fig. 8(a), the potential peak strongly decreases and the potential curve flattens during cycling for the scenario with oxygen vacancies and protons (color gradient).

During cycling in the scenario with oxygen vacancies and protons, the protons quickly move away from the top electrode due to their lower activation energy and distribute over the whole oxide and over time even accumulate at the bottom electrode [see Fig. 8(c)]. This clearly reduces the potential peak, which additionally makes it easier for the comparatively slow oxygen vacancies to move away from the top electrode [cf. Fig. 8(b)]. When only oxygen vacancies are present as mobile species, the oxygen vacancies hardly move away from the top electrode due to their higher activation energy and their initial distribution (not shown here) leads to a constantly high potential difference. It should be mentioned that simulations using a uniform distribution of oxygen vacancies close to the top electrode instead of a linearly decreasing distribution led to similar simulation results, which are not shown here. These simulation results nicely go along with the experimental findings and the model idea introduced before. We showed that the addition of protons leads to a lowering of the potential difference over the HfO_x film and, thus, to a reduction in the internal field responsible for the strong observed imprint during cycling. Consequently, in the presence of an internal field, ferroelectric switching is favored in humid atmosphere.

G. Frequency dependence and fabrication impact

Further experiments are performed to investigate the frequency dependence of the wake-up effect. When applying a frequency of 100 kHz in ambient atmosphere, similar to measurements in vacuum, no strong wake-up effect is observable for the first 2000 cycles [see Fig. 9(a)]. Unlike measurements performed at 1 kHz, the higher frequency results in the fact that the voltage is not applied long enough to redistribute protons or oxygen vacancies. As a consequence, the internal field is not reduced and no hysteresis is formed [compare inlet Fig. 9(a)]. By increasing the voltage to 8 V, which is here applied to the bottom electrode (the internal field shifts the coercive voltage to higher positive values), switching peaks are recognizable after 2000 cycles and a positive coercive voltage of 6.15 V can be extracted [Fig. 9(b)]. However, a shift of the hysteresis [inlet Figs. 9(a) and 9(b)] along the

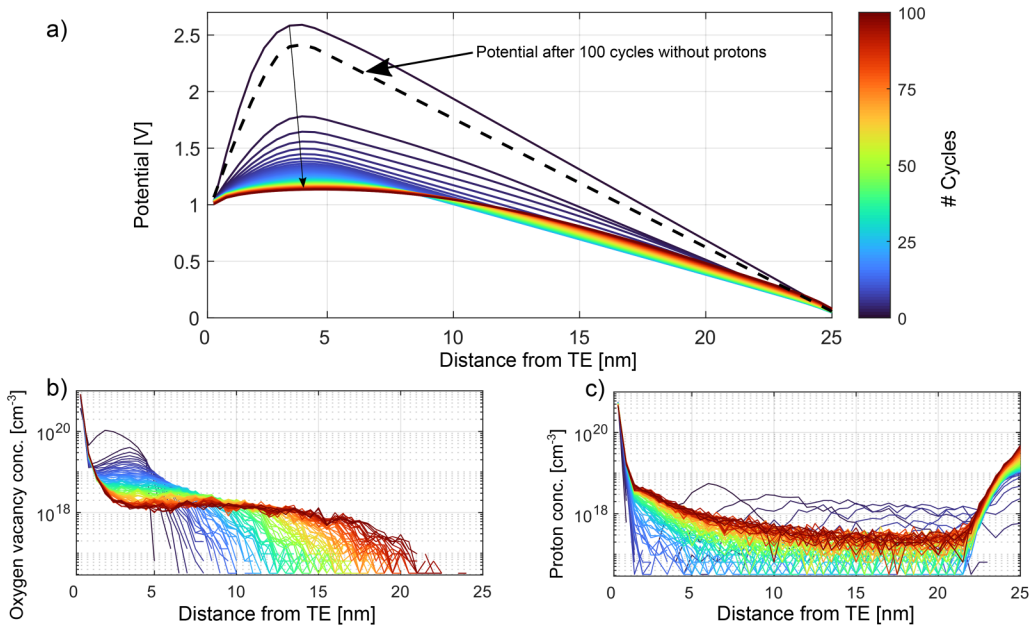

FIG. 8. (a) Potential evolution in HfO_x during cycling. The high initial potential peak is strongly reduced during cycling of the cell with oxygen vacancies and protons, whereas the effect is much lower in the simulations without protons (dashed line). In (b) and (c), the evolution of the oxygen vacancy and the proton distributions during cycling are presented.

x-axis is still observed, indicating that the internal bias field is still strongly present after 2000 cycles. This can be attributed on the one hand to the slower redistribution of protons for the higher cycling frequency (100 kHz). On the other hand, for the lower frequency (1 kHz), the moisture content was very low during the measurements, leading to the observed voltage shift. We identify a voltage shift around 2 V compared to measurements taken at 1 kHz. The results of the frequency-dependent measurements support our assumption, that moisture clearly contributes to reducing the imprint effect. The imprint effect is a common failure mechanism of ferroelectrics that results in degraded device performance. To prevent an internal field from developing that would cause the hysteresis shift along the voltage axis, the asymmetric distribution of oxygen vacancies must be suppressed. Therefore, a thin HfO_x film is deposited with the same parameters but annealed in 50% oxygen/50% nitrogen atmosphere (structural information in Fig. S7 in supplementary material). According to Ref. 22, the formation of oxygen vacancies is not so highly favored when annealing is carried out in

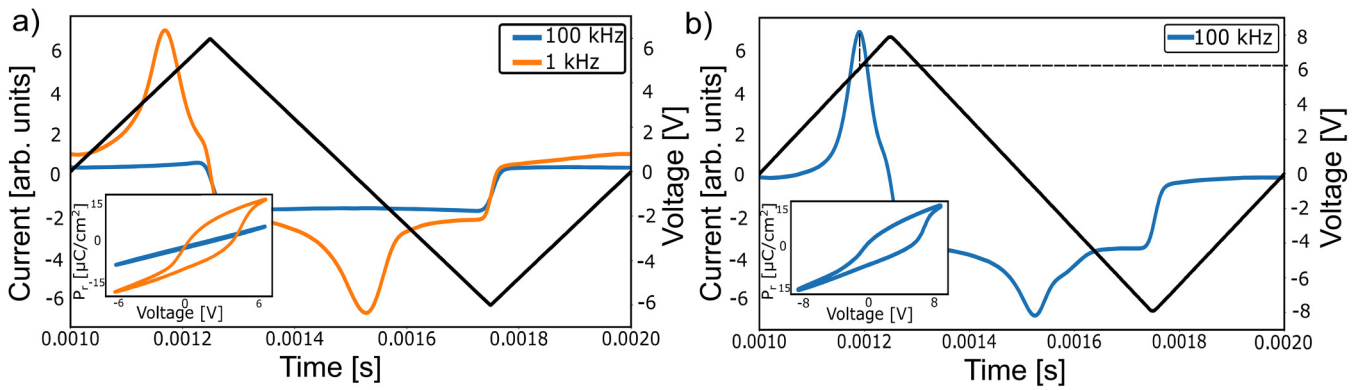

FIG. 9. (a) Measurements of the switching current taken after 2000 cycles at frequencies of 1 and 100 kHz and for an applied voltage of 6 V. In the inlet figure, the resulting polarization in the form of hysteresis is shown. (b) Switching current taken at a frequency of 100 kHz and at an increased excitation voltage of 8 V.

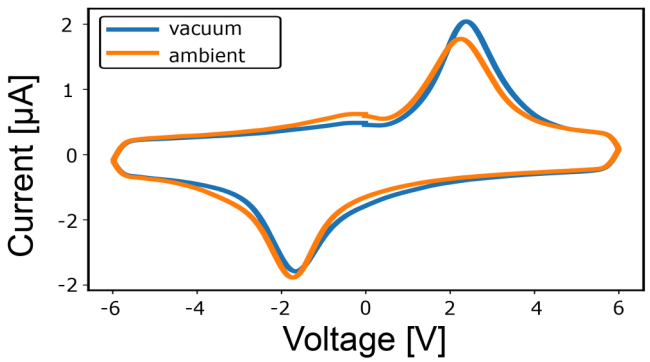

FIG. 10. Ferroelectric HfO_x thin film annealed in 50% oxygen/50% nitrogen atmosphere and measured in vacuum and in ambient atmosphere.

oxygen-rich atmospheres resulting in a lower bias field compared to samples annealed in nitrogen atmosphere. In Fig. 10, the corresponding hysteresis of the sample, which is annealed in oxygen is illustrated for measurements taken in vacuum and in ambient atmosphere after 1000 cycles. In contrast to the film annealed in nitrogen, the sample shows ferroelectric switching behavior for lower applied voltages in vacuum with comparable polarization values as in humidity and the coercive voltages are similar for vacuum and ambient atmosphere. Annealing in oxygen-rich atmosphere leads to a lowering or even preventing of the internal bias field caused during deposition.

H. Influence on conductivity

Apart from its effect on the ferroelectric behavior, moisture also affects the leakage current and the resulting conductivity.

In the literature,[21] it has been shown that OH^- can contribute to the ionic current and thus increase the total conductivity $\sigma_{total} = \sigma_{electronic} + \sigma_{ionic}$.

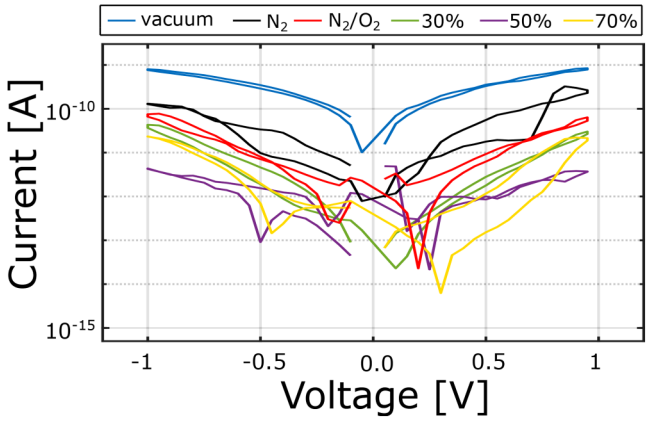

FIG. 11. Leakage current measurements of HfO_x for different atmospheres.

In this work, leakage current measurements were performed to draw conclusions about conductivity under humidity. The applied voltage was chosen to be 1 V to prevent redox peaks due to electrochemical processes, which has been reported for hafnium oxide in Ref. 45. In Fig. 11, measurements of the leakage current are shown recorded in vacuum, in dry nitrogen, in a dry nitrogen/oxygen mix (30%/70%), under 30% humidity, 50% humidity, and 70% humidity conditions. In vacuum, the film exhibits the highest leakage current. The addition of dry nitrogen slightly reduces the leakage current, and a further reduction in leakage current is observed for a mixture of dry oxygen and nitrogen.

Humid atmospheres lead to a stronger decrease in leakage current compared to vacuum, which is significant at 50% moisture. With increasing the humidity content to 70%, the leakage current increases slightly again.

The decrease in leakage current for humidity has been observed before for ZnO in Ref. 21. It is known from the literature that for the stabilization of the ferroelectric phase in undoped HfO_x, oxygen vacancies are relevant.[17,22] Furthermore, HfO_x is also used as a known resistive switching material, which is also based on the migration of oxygen vacancies.[51] Thus, it can be assumed that the hafnium oxide prepared in our work is n-doped due to the presence of oxygen vacancies. According to Ref. 21 and theoretical calculations made in Ref. 52, the incorporation of OH^- leads to the appearance of deep surface states at the top of the valence band that acts as electron traps resulting in bend bending. This results in a barrier to the current transport along the grain boundaries and in a reduction of the leakage current. For increasing amount of moisture though, more protons are incorporated into the thin film, which leads to an increase in the ionic conductivity contributing to the total conductivity and to the observed increase in leakage current for 70% humidity.

The slight decrease in leakage current under dry nitrogen and oxygen atmosphere can be attributed, on the one hand, to the increase of relative humidity to 4% and, thus, to the incorporation of OH^-. On the other hand, for the dry oxygen atmosphere, oxygen can be incorporated into the film, resulting in an annihilation of oxygen vacancies and a decrease in the leakage current. However, similar to the effect on ferroelectric properties, the effect is not as pronounced as in humid atmospheres.

IV. CONCLUSION

We presented for the first time a detailed study on the influence of different atmospheres on the ferroelectric switching behavior of undoped HfO_x thin films. At the same field strength, the wake-up effect and, thus, ferroelectric switching is suppressed in vacuum and reduced in dry atmosphere, while the film shows a remanent polarization between 13 and 25 C/cm^2 in humid atmospheres. However, ferroelectric switching in vacuum can be achieved by increasing the excitation voltage. We attribute this effect to an initial distribution of oxygen vacancies causing an internal bias field and imprint in the thin film due to nitrogen annealing. In humid atmospheres, protons can be incorporated in the thin film and lead to a decrease of the bias field due to their redistribution under the application of an electric field which reduces the imprint. KMC simulations showed that the proton

movement leads to a lowering of the potential and thus of the internal field which allows the oxygen vacancies to redistribute within the oxide layer. The level of humidity influences the duration of the wake-up effect since more incorporated protons result in a faster redistribution. Annealing in oxygen atmosphere can prevent the creation of oxygen vacancies accumulation at the interface and thus the resulting imprint effect. Additional measurements of the leakage current in different levels of humidity showed that moisture also affects the resulting conductivity.

SUPPLEMENTARY MATERIAL

See the supplementary material for Figs. S1–S7. Additional information on the direction of the internal bias field and the effect of additional heating during evacuation as well as structural information can be found in the supplementary material.

ACKNOWLEDGMENTS

This work was funded by the German Research Foundation (Deutsche Forschungsgemeinschaft) within the scope of the project "Zeppelin" (Project No. BO 1629/12).

AUTHOR DECLARATIONS

Conflict of Interest

The authors have no conflicts to disclose.

Author Contributions

Fenja Berg: Investigation (lead); Visualization (lead); Writing – original draft (lead). **Nils Kopperberg:** Investigation (supporting); Writing – original draft (supporting). **Jan Lübben:** Writing – original draft (supporting). **Ilia Valov:** Supervision (equal). **Xiaochao Wu:** Investigation (supporting); Writing – original draft (supporting). **Ulrich Simon:** Supervision (equal). **Ulrich Böttger:** Supervision (equal).

DATA AVAILABILITY

The data that support the findings of this study are available within the article and its supplementary material.

REFERENCES

[1]T. Böscke, J. Müller, D. Bräuhaus, U. Schröder, and U. Böttger, "Ferroelectricity in hafnium oxide thin films," Appl. Phys. Lett. **99**, 102903 (2011).
[2]T. Böscke, J. Müller, D. Bräuhaus, U. Schröder, and U. Böttger, "Ferroelectricity in hafnium oxide: CMOS compatible ferroelectric field effect transistors," in *2011 International Electron Devices Meeting* (IEEE, 2011), pp. 24–5.
[3]U. Schroeder, S. Mueller, J. Mueller, E. Yurchuk, D. Martin, C. Adelmann, T. Schloesser, R. van Bentum, and T. Mikolajick, "Hafnium oxide based CMOS compatible ferroelectric materials," ECS J. Solid State Sci. Technol. **2**, N69 (2013).
[4]X. Sang, E. D. Grimley, T. Schenk, U. Schroeder, and J. M. LeBeau, "On the structural origins of ferroelectricity in HfO_2 thin films," Appl. Phys. Lett. **106**, 162905 (2015).
[5]R. Materlik, C. Künneth, and A. Kersch, "The origin of ferroelectricity in $Hf_{1-x}Zr_xO$: A computational investigation and a surface energy model," J. Appl. Phys. **117**, 134109 (2015).
[6]Y. Wei, P. Nukala, M. Salverda, S. Matzen, H. J. Zhao, J. Momand, A. S. Everhardt, G. Agnus, G. R. Blake, P. Lecoeur, and B. J. Kooi, "A rhombohedral ferroelectric phase in epitaxially strained $Hf_{0.5}Zr_{0.5}O_2$ thin films," Nat. Mater. **17**, 1095–1100 (2018).
[7]P. Nukala, Y. Wei, V. de Haas, Q. Guo, J. Antoja-Lleonart, and B. Noheda, "Guidelines for the stabilization of a polar rhombohedral phase in epitaxial $Hf_{0.5}Zr_{0.5}O_2$ thin films," Ferroelectrics **569**, 148–163 (2020).
[8]D. Zhou, J. Xu, Q. Li, Y. Guan, F. Cao, X. Dong, J. Müller, T. Schenk, and U. Schröder, "Wake-up effects in Si-doped hafnium oxide ferroelectric thin films," Appl. Phys. Lett. **103**, 192904 (2013).
[9]T. Schenk, U. Schroeder, M. Pešić, M. Popovici, Y. V. Pershin, and T. Mikolajick, "Electric field cycling behavior of ferroelectric hafnium oxide," ACS Appl. Mater. Interfaces **6**, 19744–19751 (2014).
[10]M. Pešić, F. P. G. Fengler, L. Larcher, A. Padovani, T. Schenk, E. D. Grimley, X. Sang, J. M. LeBeau, S. Slesazeck, U. Schroeder, and T. Mikolajick, "Physical mechanisms behind the field-cycling behavior of HfO_2-based ferroelectric capacitors," Adv. Funct. Mater. **26**, 4601–4612 (2016).
[11]M. H. Park, H. J. Kim, Y. J. Kim, Y. H. Lee, T. Moon, K. D. Kim, S. D. Hyun, and C. S. Hwang, "Study on the size effect in $Hf_{0.5}Zr_{0.5}O_2$ films thinner than 8 nm before and after wake-up field cycling," Appl. Phys. Lett. **107**, 192907 (2015).
[12]T. Schenk, M. Hoffmann, J. Ocker, M. Pesic, T. Mikolajick, and U. Schroeder, "Complex internal bias fields in ferroelectric hafnium oxide," ACS Appl. Mater. Interfaces **7**, 20224–20233 (2015).
[13]S. Starschich, S. Menzel, and U. Böttger, "Evidence for oxygen vacancies movement during wake-up in ferroelectric hafnium oxide," Appl. Phys. Lett. **108**, 032903 (2016).
[14]P. Buragohain, C. Richter, T. Schenk, H. Lu, T. Mikolajick, U. Schroeder, and A. Gruverman, "Nanoscopic studies of domain structure dynamics in ferroelectric La: HfO_2 capacitors," Appl. Phys. Lett. **112**, 222901 (2018).
[15]F. P. Fengler, M. Pešić, S. Starschich, T. Schneller, U. Böttger, T. Schenk, M. H. Park, T. Mikolajick, and U. Schroeder, "Comparison of Hafnia and PZT based ferroelectrics for future non-volatile fram applications," in *2016 46th European Solid-State Device Research Conference (ESSDERC)* (IEEE, 2016), pp. 369–372.
[16]F. Huang, X. Chen, X. Liang, J. Qin, Y. Zhang, T. Huang, Z. Wang, B. Peng, P. Zhou, H. Lu, and L. Zhang, "Fatigue mechanism of yttrium-doped hafnium oxide ferroelectric thin films fabricated by pulsed laser deposition," Phys. Chem. Chem. Phys. **19**, 3486–3497 (2017).
[17]T. Mittmann, M. Michailow, P. D. Lomenzo, J. Gärtner, M. Falkowski, A. Kersch, T. Mikolajick, and U. Schroeder, "Stabilizing the ferroelectric phase in HfO_2-based films sputtered from ceramic targets under ambient oxygen," Nanoscale **13**, 912–921 (2021).
[18]M. Materano, P. D. Lomenzo, A. Kersch, M. H. Park, T. Mikolajick, and U. Schroeder, "Interplay between oxygen defects and dopants: Effect on structure and performance of HfO_2-based ferroelectrics," Inorg. Chem. Front. **8**, 2650–2672 (2021).
[19]U. Schroeder, M. Materano, T. Mittmann, P. D. Lomenzo, T. Mikolajick, and A. Toriumi, "Recent progress for obtaining the ferroelectric phase in hafnium oxide based films: Impact of oxygen and zirconium," Jpn. J. Appl. Phys. **58**, SL0801 (2019).
[20]M. Lederer, P. Bagul, D. Lehninger, K. Mertens, A. Reck, R. Olivo, T. Kampfe, K. Seidel, and L. M. Eng, "Influence of annealing temperature on the structural and electrical properties of Si-doped ferroelectric hafnium oxide," ACS Appl. Electron. Mater. **3**, 4115–4120 (2021).
[21]G. Milano, M. Luebben, M. Laurenti, S. Porro, K. Bejtka, S. Bianco, U. Breuer, L. Boarino, I. Valov, and C. Ricciardi, "Ionic modulation of electrical conductivity of ZnO due to ambient moisture," Adv. Mater. Interfaces **6**, 1900803 (2019).
[22]F. Berg, J. Lübben, and U. Böttger, "Parameters for ferroelectric phase stabilization of sputtered undoped hafnium oxide thin films," Jpn. J. Appl. Phys. **62**, 015507 (2023).
[23]Q. Ma, H. He, and Y. Liu, "In situ DRIFTS study of hygroscopic behavior of mineral aerosol," J. Environ. Sci. **22**, 555–560 (2010).
[24]P. Kubelka and F. Munk, "An article on optics of paint layers," Z. Tech. Phys. **12**, 259–274 (1931).

[25]M. Milosevic and S. Berets, "A review of FT-IR diffuse reflection sampling considerations," Appl. Spectrosc. Rev. **37**(4), 347–364 (2002).
[26]M. Lucarini, A. Durazzo, J. Kiefer, A. Santini, G. Lombardi-Boccia, E. B. Souto, A. Romani, A. Lampe, S. Ferrari Nicoli, P. Gabrielli, and N. Bevilacqua, "Grape seeds: Chromatographic profile of fatty acids and phenolic compounds and qualitative analysis by FTIR-ATR spectroscopy," Foods **9**, 10 (2019).
[27]S. Chemchoub, L. Oularbi, A. El Attar, S. A. Younssi, F. Bentiss, C. Jama, and M. El Rhazi, "Cost-effective non-noble metal supported on conducting polymer composite such as nickel nanoparticles/polypyrrole as efficient anode electrocatalyst for ethanol oxidation," Mater. Chem. Phys. **250**, 123009 (2020).
[28]M. M. Frank, S. Sayan, S. Dörmann, T. J. Emge, L. S. Wielunski, E. Garfunkel, and Y. J. Chabal, "Hafnium oxide gate dielectrics grown from an alkoxide precursor: Structure and defects," Mater. Sci. Eng., B **109**, 6–10 (2004).
[29]A. Rastorguev, V. Belyi, T. Smirnova, L. Yakovkina, M. Zamoryanskaya, V. Gritsenko, and H. Wong, "Luminescence of intrinsic and extrinsic defects in hafnium oxide films," Phys. Rev. B **76**, 235315 (2007).
[30]D. Neumayer and E. Cartier, "Materials characterization of ZrO_2–SiO_2 and HfO_2–SiO_2 binary oxides deposited by chemical solution deposition," J. Appl. Phys. **90**, 1801–1808 (2001).
[31]T. Szyjka, L. Baumgarten, T. Mittmann, Y. Matveyev, C. Schlueter, T. Mikolajick, U. Schroeder, and M. Muller, "Enhanced ferroelectric polarization in tin/HfO_2/TiN capacitors by interface design," ACS Appl. Electron. Mater. **2**, 3152–3159 (2020).
[32]W. Hamouda, F. Mehmood, T. Mikolajick, U. Schroeder, T. O. Mentes, A. Locatelli, and N. Barrett, "Oxygen vacancy concentration as a function of cycling and polarization state in TiN/$Hf_{0.5}Zr_{0.5}O_2$2/TiN ferroelectric capacitors studied by x-ray photoemission electron microscopy," Appl. Phys. Lett. **120**, 202902 (2022).
[33]M. Copel, R. P. Pezzi, D. Neumayer, and P. Jamison, "Reduction of hafnium oxide and hafnium silicate by rhenium and platinum," Appl. Phys. Lett. **88**, 072914 (2006).
[34]G. Milano, M. Luebben, M. Laurenti, L. Boarino, C. Ricciardi, and I. Valov, "Structure-dependent influence of moisture on resistive switching behavior of ZnO thin films," Adv. Mater. Interfaces **8**, 2100915 (2021).
[35]I. Valov and T. Tsuruoka, "Effects of moisture and redox reactions in VCM and ECM resistive switching memories," J. Phys. D: Appl. Phys. **51**, 413001 (2018).
[36]S. Kim, H. J. Avila-Paredes, S. Wang, C.-T. Chen, R. A. De Souza, M. Martin, and Z. A. Munir, "On the conduction pathway for protons in nanocrystalline yttria-stabilized zirconia," Phys. Chem. Chem. Phys. **11**, 3035–3038 (2009).
[37]A. Marinopoulos, "Protons in cubic yttria-stabilized zirconia: Binding sites and migration pathways," Solid State Ionics **315**, 116–125 (2018).
[38]S. Menzel, M. Von Witzleben, V. Havel, and U. Böttger, "The ultimate switching speed limit of redox-based resistive switching devices," Faraday Discuss. **213**, 197–213 (2019).
[39]S. Zafar, H. Jagannathan, L. F. Edge, and D. Gupta, "Measurement of oxygen diffusion in nanometer scale HfO_2 gate dielectric films," Appl. Phys. Lett. **98**, 152903 (2011).
[40]R. He, H. Wu, S. Liu, H. Liu, X. R. Wang, and Z. Zhong, "Charged oxygen vacancy induced ferroelectric structure transition in hafnium oxide," arXiv:2106.12159 (2021).
[41]N. Kopperberg, S. Wiefels, S. Liberda, R. Waser, and S. Menzel, "A consistent model for short-term instability and long-term retention in filamentary oxide-based memristive devices," ACS Appl. Mater. Interfaces **13**, 58066–58075 (2021).
[42]J. Hinterberg, A. Adams, B. Blümich, P. Heitjans, S. Kim, Z. A. Munir, and M. Martin, "1 H-NMR measurements of proton mobility in nano-crystalline YSZ," Phys. Chem. Chem. Phys. **15**, 19825–19830 (2013).
[43]M. Takayanagi, S. Furuichi, W. Namiki, T. Tsuchiya, M. Minohara, M. Kobayashi, K. Horiba, H. Kumigashira, and T. Higuchi, "Proton conduction on YSZ electrolyte thin films prepared by RF magnetron sputtering," ECS Trans. **75**, 115 (2017).
[44]R. Merkle and J. Maier, "How is oxygen incorporated into oxides? A comprehensive kinetic study of a simple solid-state reaction with $SrTiO_3$ as a model material," Angew. Chem. Int. Ed. **47**, 3874–3894 (2008).
[45]M. Lübben, S. Wiefels, R. Waser, and I. Valov, "Processes and effects of oxygen and moisture in resistively switching TaO_x and HfO_x," Adv. Electron. Mater. **4**, 1700458 (2018).
[46]J. Schaeffer, L. Fonseca, S. Samavedam, Y. Liang, P. Tobin, and B. White, "Contributions to the effective work function of platinum on hafnium dioxide," Appl. Phys. Lett. **85**, 1826–1828 (2004).
[47]R. P. Pezzi, M. Copel, M. Gordon, E. Cartier, and I. J. R. Baumvol, "Oxygen transport and reaction mechanisms in rhenium gate contacts on hafnium oxide films on Si," Appl. Phys. Lett. **88**, 243509 (2006).
[48]E. D. Grimley, T. Schenk, X. Sang, M. Pešić, U. Schroeder, T. Mikolajick, and J. M. LeBeau, "Structural changes underlying field-cycling phenomena in ferroelectric HfO_2 thin films," Adv. Electron. Mater. **2**, 1600173 (2016).
[49]N. Kopperberg, S. Wiefels, K. Hofmann, J. Otterstedt, D. J. Wouters, R. Waser, and S. Menzel, "Endurance of 2 Mbit based BEOL integrated ReRAM," IEEE Access **10**, 122696–122705 (2022).
[50]C. La Torre, A. F. Zurhelle, T. Breuer, R. Waser, and S. Menzel, "Compact modeling of complementary switching in oxide-based ReRAM devices," IEEE Trans. Electron Devices **66**, 1268–1275 (2019).
[51]W. Banerjee, A. Kashir, and S. Kamba, "Hafnium oxide (HfO_2)—A multifunctional oxide: A review on the prospect and challenges of hafnium oxide in resistive switching and ferroelectric memories," Small **18**, 2107575 (2022).
[52]S. Porro, F. Risplendi, G. Cicero, K. Bejtka, G. Milano, P. Rivolo, A. Jasmin, A. Chiolerio, C. F. Pirri, and C. Ricciardi, "Multiple resistive switching in core–shell ZnO nanowires exhibiting tunable surface states," J. Mater. Chem. C **5**, 10517–10523 (2017).